First publ. in: Photochemistry and Photobiology 76 (2002), 5, pp. 501–508

New Insights into Photosynthetic Oscillations Revealed by Two-dimensional Microscopic Measurements of Chlorophyll Fluorescence Kinetics in Intact Leaves and Isolated Protoplasts¶

Naila Ferimazova[1,2], Hendrik Küpper*[1,2,3], Ladislav Nedbal[1,4] and Martin Trtílek[5]

[1]Faculty of Biological Sciences and Institute of Physical Biology, University of South Bohemia, České Budejovice, Czech Republic;
[2]Department of Autotrophic Microorganisms, Institute of Microbiology ASCR, Třeboň, Czech Republic;
[3]Fachbereich Biologie, Mathematisch-Naturwissenschaftliche Sektion, Universität Konstanz, Konstanz, Germany;
[4]Laboratory of Applied Photobiology and Bio-Imaging, Institute of Landscape Ecology ASCR, Nové Hrady, Czech Republic and
[5]Photon Systems Instruments Ltd., Brno, Czech Republic

Received 19 March 2002; accepted 12 August 2002

ABSTRACT

Chlorophyll fluorescence kinetic microscopy was used to analyze photosynthetic oscillations in individual cells of leaves and in isolated leaf cell protoplasts. Four Brassicaceae species were used: *Arabidopsis halleri* (L.) O'Kane & Al-Shehbaz, *Thlaspi fendleri* (Nels.) Hitchc, *Thlaspi caerulescens* J.&C. Presl and *Thlaspi ochroleucum* Boiss et Helder. With the latter two, the measurements were extended also to isolated protoplasts. The oscillations were induced under the microscope by exposing dark-adapted samples to actinic irradiance. Detailed analysis of the induced transients revealed that they consist of several processes oscillating with different frequencies and not only one component as reported earlier. Furthermore, it was found that most of these processes are controlled inside each individual cell. This was shown by differences in oscillations in neighboring cells and protoplasts that share a uniform intercellular environment. The frequency of the dominant oscillation frequency depended neither on irradiance nor on CO_2 concentration and is, therefore, not controlled by the photosynthetic rate. Characteristic differences in the frequency spectrum and damping of oscillations have been found among the plant species examined.

INTRODUCTION

Oscillations of photosynthesis have been reported as early as 1949 by Van der Veen, who already demonstrated their dependence on irradiance, temperature and oxygen concentration (1,2). The oscillations have been used since then as a valuable tool providing original insight into photosynthetic mechanisms and regulation (for reviews see references [3–5]).

Two approaches were used for studying oscillations. (1) Experiments were carried out with diverse plant species under various conditions to find oscillating parameters of cell metabolism and to find out which conditions are inducing oscillations (1,2,6–13). (2) In a complementary approach, theoretical models of oscillatory processes were constructed to explain the experimental data and to predict novel properties of photosynthetic oscillations (14–19). Among the most frequently proposed mechanisms for short period oscillations (10–120 s) one can find an imbalance in the supply of adenosine triphosphate (ATP) and reduced nicotinamide adenine dinucleotide phosphate to the Calvin cycle (first proposed by Ogawa [10] and first analyzed in detail by Laisk *et al.* [11]), competition for ATP between the two kinases in the Calvin cycle (9), imbalance in the fructose 2,6-bisphosphate control of the sucrose synthesis and release of inorganic phosphate (P_i) (20). More recently it has been proposed that sugar transport between mesophyll cells (14), independent changes of ATP/adenosine 5′ diphosphate and ΔpH (21) as well as changes in membrane potential related to oscillating ion fluxes (19) may play an important role in controlling the fast photosynthetic oscillations. Despite these efforts, many of the crucial questions concerning the mechanisms of photosynthetic oscillations remained open or controversial (4).

For longer period oscillations of photosynthesis (about 5–40 min), the feedback regulation of stomatal opening has been proposed by Raschke (7,22). This concept seems to be widely accepted so that much less debate exists about the mechanism of oscillations caused by stomatal movements compared with the aforementioned short-period oscillations.

Until the early 1980s mainly gas exchange was used to record photosynthetic oscillations. Later on, kinetic records of chlorophyll (Chl) fluorescence quantum yield were frequently used for this purpose (9,11,13,14). This approach was made possible because algorithms that allow us to calculate the quantum yield of PS II (photosystem II) photochemistry and of photosynthetic electron transport from fluorescence measurements have been developed (23,24). The introduction of the fluorescence technique was also

---

¶Posted on the web site on 28 August 2002.

*To whom correspondence should be addressed at: Fachbereich Biologie, Mathematisch-Naturwissenschaftliche Sektion, Universität Konstanz, Postfach M665, D-78457 Konstanz, Germany. Fax: 49-7531 88-2966; e-mail: hendrik.kuepper@web.de

Abbreviations: CCD, charge-coupled device, the light detector of digital video cameras; Chl, chlorophyll; F_0, minimal fluorescence yield of a dark adapted sample = fluorescence in nonactinic measuring light; F_m, maximum fluorescence yield of a dark-adapted sample; F_s, steady state fluorescence under the given actinic irradiance; F_v, variable fluorescence ($F_v = F_m - F_0$); F_p, fluorescence yield at the peak level of the induction curve; LED, light emitting diode; PAM, pulse amplitude modulation.

facilitated by its easy use and high time resolution. In addition, the recent development of fluorescence imaging has provided a unique possibility to demonstrate that oscillations are heterogeneous for the surface of a leaf, a result that would be impossible with the earlier integrative methods (13,14,25,26). The reasons for this heterogeneity remained largely unknown. It has been proposed in the articles quoted above that the areas of a leaf that are separated by small veins (*i.e*. the alveoli in heterobaric leaves) are the oscillating units and that the heterogeneity is caused by transport processes.

We recently developed a technique for two-dimensional fluorescence kinetic measurements and imaging at microscopic resolution, so that emission kinetics from individual chloroplasts can be studied and compared (27). We now used this instrument to analyze the heterogeneity in oscillations in various mesophyll cells for the leaf surface on the microscopic scale. In the present study, oscillations were studied in intact leaves of four species of Brassicaceae, two of them Zn–Cd hyperaccumulator plants (*Thlaspi caerulescens*: [28], *Arabidopsis halleri*: [29]). Furthermore, with *T. caerulescens* and *Thlaspi ochroleucum* the studies were also extended to isolated protoplasts of mesophyll cells to find out which oscillation parameters are determined inside the individual cells and which are controlled by cell–cell interactions.

MATERIALS AND METHODS

Plant material, culture media and culture conditions. Seeds of *A. halleri* (L.) O'Kane & Al-Shehbaz (=*Cardaminopsis halleri*), *T. caerulescens* J.&C. Presl, *Thlaspi fendleri* (Nels.) Hitchc and *T. ochroleucum* Boiss et Helder (kindly provided by the IACR Rothamsted, UK) were germinated on a mixture of perlite and vermiculite moistened with deionized water. Three weeks after germination, seedlings were transferred to 1.5 L vessels filled with a solution (Shen *et al*. [30]) containing 1000 μ*M* $Ca(NO_3)_2$, 500 μ*M* $MgSO_4$, 50 μ*M* K_2HPO_4, 100 μ*M* KCl, 10 μ*M* H_3BO_3, 0.2 μ*M* Na_2MoO_4, 0.31 μ*M* $CuSO_4$, 0.5 μ*M* $NiSO_4$, 20 μ*M* Fe(III)-EDDHA (Fe(III)-ethylenediamine-di(*o*-hydroxyphenylacetic acid), 10 μ*M* $ZnSO_4$ and 2 μ*M* (for *T. fendleri* and *T. ochroleucum*) or 0.1 μ*M* (for *T. caerulescens* and *A. halleri*) $MnSO_4$. The pH of the solution was maintained at around 6.0 with 2000 μ*M* MES (2-morpholinoethanesulphonic acid, 50% as potassium salt). The nutrient solution was aerated continuously and renewed every 5 days. Plants were grown in a controlled environment room under the following conditions: 14 h day length with a photon flux density of 60 $\mu mol \cdot m^{-2} \cdot s^{-1}$ supplied by a 1:1 mixture of ''cool white'' and OSRAM Fluora® fluorescent tubes, 24–20°C day–night temperature. Four plants of each species were grown.

Preparation of protoplasts. Protoplasts were prepared by a method based on that of Coleman *et al*. (31), from young–mature leaves of *T. caerulescens* and *T. ochroleucum*. After a cut through the lower epidermis at the lower leaf end, the epidermis was stripped off from the mesophyll using watchmaker's forceps. Afterward, the leaves were put, with the stripped surface downward, into isolation medium (800 m*M* sorbitol, 1.0 m*M* $CaCl_2$, 10 m*M* MES, adjusted to pH 5.6 with bis-tris-propane). Once all leaves to be used for the experiment were stripped, the digestion medium (isolation medium plus 0.7% Cellulysin, 0.4% Macerase, 0.002% Pectolyase and 1% BSA) was added (same volume as isolation medium), and the sample was incubated on a shaker. The whole procedure was carried out at room temperature. When the walls of the mesophyll cells were completely digested, usually after 8–16 h of incubation (depending on leaf age and species), the remaining upper epidermis was removed and the protoplast suspension was either used immediately or stored at 4°C in the refrigerator. The protoplasts remained fully active for up to 16 h of storage.

Preparation of samples for measurements. A young–mature leaf was cut off from the plant and mounted, upper side toward the glass, in the measuring chamber (standard version described by Küpper *et al*. [27]) using wet gas–permeable cellophane (as commonly used for polarographic oxygen measurements using the Clark-type electrode). This kind of preparation kept the petiole in water. The chamber was kept at room temperature that was about 20°C and was ventilated by a stream of gas (2 $L \cdot min^{-1}$), which was maintained at 20°C and saturated with water vapor at this temperature, thus preventing the leaf from drying during the measurement. Water saturation was reached by pressing gas through fine pores of a diffusor under water at about 25°C and then cooling the gas down to 20°C, where the surplus humidity condensed. Using a gas mixer, the contents of O_2, N_2 and CO_2 in this stream of gas were smoothly variable from 0–100%.

For measuring protoplasts, 50 μL of the protoplast suspension was mixed on the inner surface of the glass window of the measuring chamber (high version [27])) with 100 μL of 2% ultralow-gelling (25°C) agarose in isolation medium (see above). Immediately after adding the agarose, the mixture was covered with gas-permeable cellophane (previously soaked in isolation medium at 20°C) and stretched by an o-ring. The gas-permeability of the cellophane was proven by replacing it with a plastic net, which yielded the same results as the cellophane. A stream of temperature-controlled (20°C) isolation medium was passed through the chamber at a rate of about 50 $mL \cdot min^{-1}$ using a centrifugal pump. The medium was kept in equilibrium with the desired gas mixture by aerating it in the circulation reservoir placed in a thermostat.

For measuring the dependence of oscillations on gas conditions or irradiance (or both), the same leaf was treated with all conditions to be tested, with 10 min breaks for readaptation to the dark state in between. In this way, the treatment-specific effect could be easily distinguished from differences between individual leaves–protoplast preparations. Each experiment (=series of measurements) was replicated at least three times, each time with a fresh leaf–protoplast sample, to check the reproducibility of the results.

Chlorophyll fluorescence measurements. Photosynthetic performance of tissues and protoplasts was measured using the fluorescence kinetic microscope as described by Küpper *et al*. (27) and produced by Photon Systems Instruments (Brno, Czech Republic) with the following modifications. (1) Nonactinic measuring light (F_0) was produced by a xenon flash lamp equipped with a set of filters to produce a spectrum similar to the earlier used light emitting diode (LED). The resulting measuring light irradiance was about 0.2 $\mu mol \cdot m^{-2} \cdot s^{-1}$ at 3 Hz, which was the flash repetition rate for the F_0 and F_0' measurements. (2) Because the fluorescent signal was strong enough, a sensitive, nonintensified charge-coupled device camera (the camera of the ''FluorCam'' system (version 700M) from Photon Systems Instruments) was used instead of the intensified one, resulting in an improved spatial resolution and decreased noise.

The measurements were performed with an automatic subtraction of background signals and a maximum time resolution of 80 ms. In the slower parts of the kinetics, lower time resolution was applied. Each image of the resulting fluorescence kinetic records had a resolution of 300 × 400 pixels at 8 bits.

Analysis of fluorescence kinetic records. The original two-dimensional data, *i.e*. films of Chl fluorescence kinetics, were analyzed using the FluorCam software from Photon Systems Instruments in the following way. Images of maximum fluorescence yield of a dark-adapted sample (F_m), F_0, steady state fluorescence under the given actinic irradiance (F_s), variable fluorescence ($F_v = F_m - F_0$), $(F_v)/F_m$, *etc*. were generated as described in detail earlier (27). A two-dimensional map reflecting the oscillation amplitudes was constructed as a pixel-to-pixel ratio between the image taken at the maximum and the image taken at the subsequent minimum of the first period of the photosynthetic oscillations visible in the average kinetic trace. The heterogeneity visible on these images was used to select cells for further analysis. The selected cells were passed again through the analysis routine, which resulted in fluorescence kinetic traces representing the average of the kinetics of all pixels within the chosen objects. The individual kinetic traces obtained in this way were exported for further numerical analysis.

Analysis of oscillation parameters. The fluorescence kinetic traces obtained as described above were imported into both SPSS SigmaPlot® and Microcal Origin® software. The fluorescence kinetic data were then reduced to the time interval of the actinic light exposure that induced the photosynthetic oscillations, *i.e*. the data before the first oscillation peak and after switching off the actinic light were deleted. The resulting data sets were fitted in SigmaPlot® with three damped oscillations with a nonharmonic background consisting of an offset and of an exponentially decaying signal:

$$F(t) = y_0 + A_e \exp\left(-\frac{t - t_0}{\tau_e}\right) + \sum_{i=1}^{i=3} A_i \exp\left(-\frac{t - t_0}{\tau_i}\right) \sin(\omega_i t + \varphi_i)$$

where F = fluorescence, t = time, y_0 = offset constant, t_0 = starting time

of the actinic light exposure, A_e = amplitude of the exponential background, τ_e = decay time of the exponential background, A_i = amplitude of the harmonic component, τ_i = damping time of the harmonic component, ω_i = frequency of the harmonic component and φ_i = phase of the harmonic component.

In this way, we were able to separate the nonharmonic background from the harmonically modulated components of the fluorescence kinetics that was roughly fitted by the three damped sine-functions. The calculated non-harmonic background was subtracted from the measured data and the resulting harmonically modulated transient was submitted to the FFT analysis by the Origin® software.

RESULTS

The appearance of persistent, autonomous photosynthetic oscillations was first observed during microscopic measurements on *T. caerulescens* plants grown for a study of metal physiology. In contrast to many earlier studies of photosynthetic oscillations, here they turned out to be highly reproducible, so that we continued with a systematic analysis including other taxonomically related plants belonging to the same experiments. In this way, the present study became the first one analyzing photosynthetic oscillations in metal hyperaccumulator plants. Furthermore, it is one of few studies where persistent, autonomous photosynthetic oscillations were observed in ambient air.

Dark-adapted (10 min) leaves or protoplasts (see below) were first exposed to a saturating pulse of light to capture an image of F_m emission (Fig. 1). The F_m measurement was conducted to allow for a comparison with fluorescence yield at the peak level during actinic irradiance (F_p) and to assess how far the light was saturating to the sample. After 100 s dark relaxation, actinic light was switched on, inducing the Kautsky effect. Instead of the usual relaxation toward the final steady-state level, we observed, on a long time scale, a complex periodic pattern consisting of several harmonic components appearing with largely different damping constants (Fig. 1). The fluorescence emission transients were resolved down to individual cells that are represented by separate transients in Fig. 1. Subjected to analysis by Fast Fourier Transform (FFT), the oscillatory part of the fluorescence transient yielded spectra of frequency *vs* amplitude (see inserts in Fig. 1).

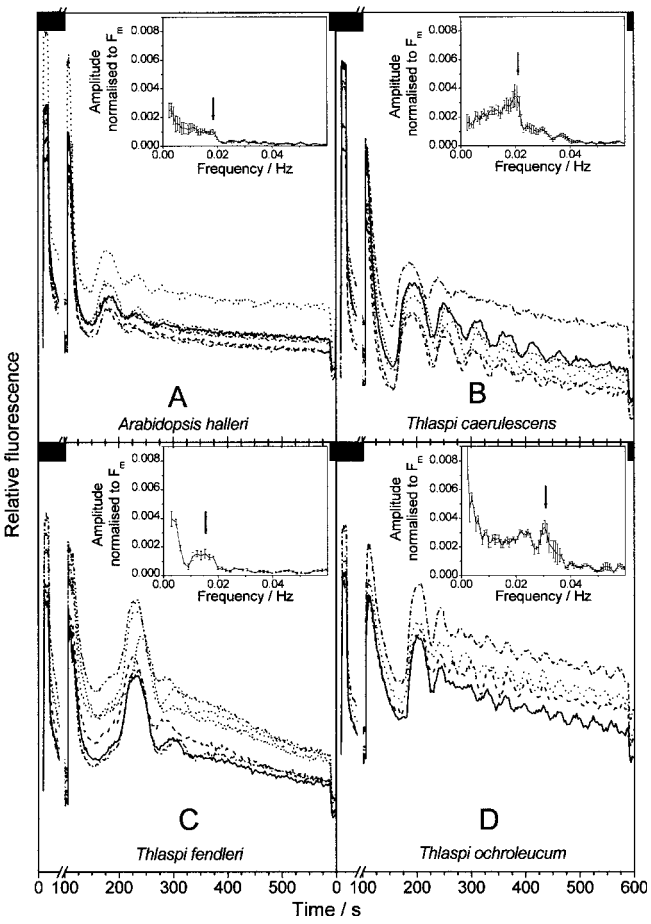

Figure 1. Comparison of oscillatory fluorescence transients in selected palisade mesophyll cells of typical mature leaves of four plant species. Individual kinetic traces show cell-to-cell variability of the transients in the selected leaf. The oscillations were measured in water-saturated air without CO_2 enrichment. Each record starts with an F_m measurement followed by 100 s dark relaxation (indicated by the black box in the left-top corner of each graph). Afterwards, the plants were exposed to actinic irradiance that elicited the oscillatory transients. The insets in each panel show the FFT frequency spectra of the oscillatory part of the respective fluorescence transient (after removal of offset and exponential trend). The line represents the average and the vertical bars show the standard errors between the cells. The arrows in the FFT inserts indicate the dominant (edge) frequency. (A) *A. halleri*, 280 $\mu mol \cdot m^{-2} \cdot s^{-1}$, (B) *T. caerulescens*, 180 $\mu mol \cdot m^{-2} \cdot s^{-1}$, (C) *T. fendleri*, 180 $\mu mol \cdot m^{-2} \cdot s^{-1}$ and (D) *T. ochroleucum*, 180 $\mu mol \cdot m^{-2} \cdot s^{-1}$. The actinic irradiances were selected for an optimum induction of oscillations, and this optimum irradiance was higher for *A. halleri* than for the other plants species.

Oscillations in intact leaves

Comparison of plant species. A comparison of different plant species showed that the dominant frequency of the oscillations was between 0.015 and 0.03 Hz in all species (kinetic plots in Fig. 1). The most obvious difference between species was the extent of damping of the oscillations and the resulting frequency spectrum (FFT inserts in Fig. 1). Whilst in *T. caerulescens* (Fig. 1B) and *T. ochroleucum* (Fig. 1D) the high frequency oscillations often persisted for more than 10 periods, in *A. halleri* at most three periods (Fig. 1A) and in *T. fendleri* at most two periods were observable (Fig. 1C). This became very obvious also in the FFT spectra (inserts of Fig. 1), where in the case of *A. halleri* and *T. fendleri* the strong damping led to broad peaks and small amplitudes of all frequencies above 0.005 Hz. In contrast, in *T. caerulescens* and *T. ochroleucum* the edge (=dominant) frequency of 0.02–0.03 Hz often represented the maximum amplitude in the frequency spectrum.

All parameters described in the following paragraphs were studied in detail only with *T. caerulescens* and *T. ochroleucum* because only in these cases the oscillations could be reliably and accurately quantified. In *A. halleri* and *T. fendleri* the damping was too strong for carrying out this task. In the case of the latter species these parameters could only be analyzed qualitatively, but the effects were in principle the same also in these species.

Frequency spectrum analysis. To check whether the high number of harmonic components detected by FFT in fluorescence transients of *T. caerulescens* and *T. ochroleucum* (Fig. 1B,D) reflect the real situation, an alternative analysis was performed on some examples as shown in Fig. 2. FFT was only used to identify the dominant frequency of the fluorescence transient (Fig. 2A, vertical line in the insert). A component of this frequency and two further components that were well visible in the FFT were fitted to the data using the equation described in Materials and Methods. In this way, damping and phase of the dominant component were determined. The resulting harmonic function (dashed line in Fig. 2A) was subtracted from the experimental data together with

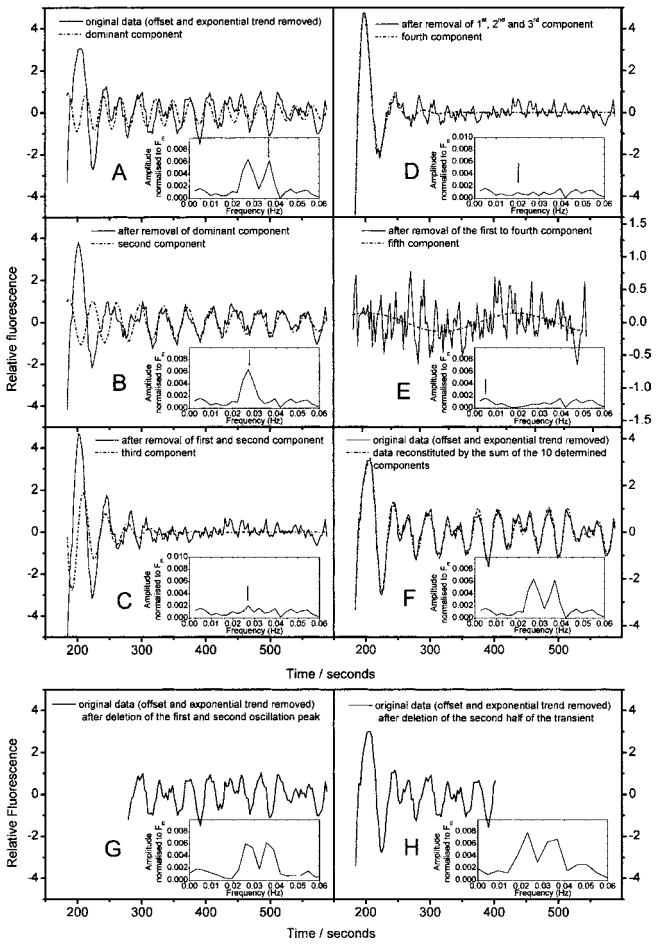

Figure 2. Alternative analysis of oscillatory fluorescence transients by sequentional fitting with damped harmonic functions, proving that many frequencies contribute to photosynthetic oscillations. The data are from a palisade mesophyll cell in a leaf of *T. ochroleucum* exposed to 180 $\mu mol \cdot m^{-2} \cdot s^{-1}$. The solid line in (A) shows the original data from which a nonoscillatory background was subtracted as described in Materials and Methods. FFT (see insets) was used to identify the frequency of the dominant (arrow in the FFT insert in (A)) and two further harmonic components. These frequencies were used to fit the data with three harmonic components of variable damping and phase in order to obtain the damping, phase and frequency of the dominant component. These parameters of the dominant component, which is shown by the dotted line in (A), were used to subtract it from the data. The residual (solid line in B) was again subjected to FFT to find the frequency of the second harmonic component (arrow in the (B) insert). Its damping and phase were determined again by fitting. Repeating this algorithm, 10 components were identified (C–E). Panel (F) shows a reconstitution (simulation) of the original data by using the 10 determined oscillation frequencies (dotted line) in comparison with the original data. Note that the FFT spectrum of this simulated curve also (small inset graph in (F)) is almost identical to the FFT spectrum of the original data (inset in (A)). Panel (G) shows the FFT analysis after deleting the first two oscillation peaks in the kinetics. Similarly, in panel (H) the second half of the kinetics was deleted before calculating the FFT.

background. The residue (solid line in Fig. 2B) was reanalyzed by FFT to determine phase and damping of a second harmonic component (Fig. 2B, vertical line in the insert). This whole procedure was repeated (Fig. 2C–E) until no significant ($P < 0.01$) oscillations remained in the residues or until ten components were identified. Fig. 2F compares the raw data after background subtraction (solid line) with the result of 10-fold fitting that yielded 10 damped harmonics. The remaining very small peaks in the FFT are most likely caused by stray light from neighboring cells.

These analyses proved several important facts:

(1) Several harmonic components contributed to the observed oscillations of fluorescence kinetics of single cells. Although the present study was focused on the short-period (<90 s) photosynthetic oscillations, the 500 s actinic light exposure was sufficient to indicate the involvement of slow components too (*e.g.* Fig. 2E, right FFT graph of Fig. 7).
(2) The dominant frequency in the FFT spectrum does not necessarily produce the highest amplitude in the fluorescence kinetics (Fig. 2A *vs* 2C,D).
(3) Strongly damped frequencies can yield very unsharp peaks hardly detectable in the FFT spectrum of the whole transient (Fig. 2C,D inserts).

Removing parts of the original data, *i.e.* either the first two oscillation peaks or the last part of the transient or both, influenced the FFT spectrum as shown in Fig. 2G,H.

(1) Removing the first two oscillation peaks had hardly any effect on the FFT spectrum (Fig. 2G) because the damped frequencies causing the high amplitude of the first peak anyway contributed only very little to the FFT spectrum of the full transient (see above; Fig. 2C,D).
(2) The amplitudes of the peaks representing the most strongly damped frequencies (shown in Fig. 2C,D) were increased in the FFT spectrum if the later part of the kinetics, where these oscillations had damped out, was deleted (Fig. 2A *vs* H). Under these conditions, the strongly damped frequencies led to very unsharp wide peaks in the FFT spectrum that may lead to a wrong estimation of neighboring frequencies.
(3) The exact positions of the frequency peaks slightly varied upon the removal of larger parts of the kinetics (Fig. 2A *vs* 2H). This indicates a shift of frequencies during the fluorescence kinetics.

Heterogeneity of oscillations for the leaf surface. The two-dimensional microscopic measurements revealed a strongly heterogeneous distribution of oscillations among leaf cells (Fig. 3). Cells less than 100 μm apart often exhibited a phase shift of more than 90° (Fig. 3A), and nonoscillating cells were found next to strongly oscillating ones (Fig. 3B). Under these conditions, an averaging of the fluorescence transients of a few cells already caused most of the oscillations to cancel out each other. The heterogeneity was always so strong that macro-imaging (resolution around 2 mm; [32]) or integrative pulse amplitude modulation (PAM) fluorometry failed to detect any macroscopic oscillations (not shown).

The extent of heterogeneity strongly varied with the irradiance. At the lowest irradiances that are sufficient to induce visible oscillations, maximum heterogeneity was observed, which decreased toward the higher irradiances. In Fig. 4 the heterogeneity is shown at a medium irradiance close to the optimum for the induction of oscillations and at a high irradiance almost saturating photosynthesis.

Impact of irradiance and gas composition. The influence of actinic light intensity was found to be connected to the gas composition during the measurement. Figure 5 shows an example for which *T. caerulescens* was used; in principle the same was also

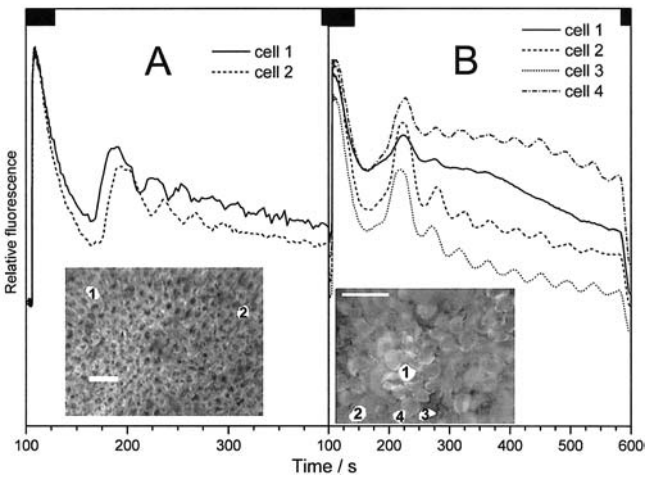

Figure 3. Spatial heterogeneity of photosynthetic oscillations in the palisade mesophyll of mature *Thlaspi* leaves. The inserts show fluorescence emission (F_p) of leaf cells (the white bars represent 100 μm). Numbers label selected cells that are represented by kinetic traces. The kinetic traces are normalized to F_m. (A) Transients of *T. ochroleucum* cells less than 500 μm apart reveal phase variability of the oscillations. (B) Transients of four *T. caerulescens* cells demonstrate large differences in damping.

found in all other species. As mentioned in Materials and Methods, the dependence of oscillations on gas conditions or irradiance (or both) was measured by treating the same leaf with all conditions to be tested, with 10 min breaks for readaptation to the dark state in between. In this way, the treatment-specific effect could be easily distinguished from differences between individual leaves. During such a series of measurements, the leaf was first exposed to a very low actinic irradiance of <40 μmol·m^{-2}·s^{-1} corresponding to less than 10% of the irradiance saturating photosynthesis (as measured by the F_p/F_m ratio). The plant responded by a fluorescence transient (Fig. 5A) with no obvious oscillatory pattern and the P-peak of the Kautsky effect that was not followed by an M-peak. The transient was not affected by increasing the CO_2 concentration from 0.03 to 1% (not shown). When a medium irradiance (~50–150 μmol·m^{-2}·s^{-1}) was applied at ambient air CO_2 concentration, an M-peak appeared about 100–150 s after the P-peak, followed by a nonoscillatory relaxation toward a steady state level (Fig. 5B). At about 150–500 μmol·m^{-2}·s^{-1} in air, the M-peak was followed by distinct oscillations (Fig. 5C–E). The irradiance leading to oscillations of highest amplitude and lowest damping was around 200–250 μmol·m^{-2}·s^{-1} in air (Fig. 5D). The dominant frequency of the oscillations was not changing with the irradiance; different irradiances only lead to differences in damping and maximum amplitude of the oscillations (Fig. 5C–E). In air enriched by 1% CO_2, the threshold of the aforementioned effects was shifted toward higher irradiance. At 1% CO_2, actinic irradiance of 300–400 μmol·m^{-2}·s^{-1} was needed to induce maximum oscillations. Although at these CO_2 levels the oscillations at their optimum irradiance were slightly stronger (higher amplitude and less damping) than in air (data not shown), CO_2 concentrations higher than 1% damped the oscillations (Fig. 6). Furthermore, increasing CO_2 concentrations led to a faster onset of the oscillations after the beginning of actinic irradiance (Fig. 6, upper panel) and to an increase in the visible oscillation frequency. The FFT spectra showed that this was not caused by a shift of any peak in the frequency spectra but by a change in the amplitude of the individual components (Fig. 6, lower panel).

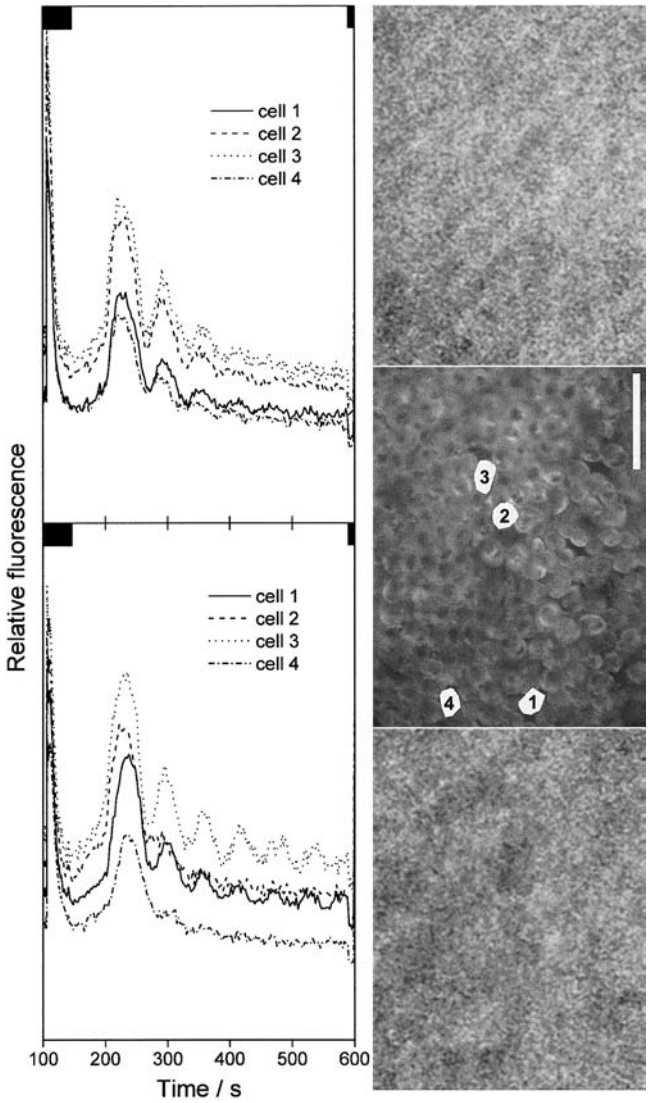

Figure 4. The cell-to-cell heterogeneity of the oscillations depends on irradiance. Four cells of palisade mesophyll of a mature leaf of *T. ochroleucum* were measured in 280 μmol·m^{-2}·s^{-1} (top) and 180 μmol·m^{-2}·s^{-1} (bottom). The fluorescence image in the middle serves to identify the palisade mesophyll cells that were analyzed for the kinetics. The white bars in the middle image represent 100 μm. The images (top: 280 μmol·m^{-2}·s^{-1}; bottom: 180 μmol·m^{-2}·s^{-1}) next to the curves display the ratio between the first oscillation peak and the next valley in the averaged fluorescence transient.

Oscillations in protoplasts

Comparison with leaves, heterogeneity among protoplasts. In general, oscillations in protoplasts were less reproducible than in leaves and were found only in fully intact protoplasts, as judged from both their outer appearance and photosynthetic performance. Oscillating protoplasts displayed the same kind of heterogeneity as cells inside leaves. They did not oscillate in synchrony, but strong phase shifts between individual protoplasts as well as differences in oscillation frequency and damping could be observed (Fig. 7A). The frequency spectrum of oscillations in protoplasts differed from that of oscillations in leaves. In most cases the oscillations in protoplasts had a lower oscillation edge frequency (dominant frequency about 0.01 Hz, Fig. 7B) than in cells of intact leaves in the same plant (0.02–0.03 Hz, Figs. 1B and 5D).

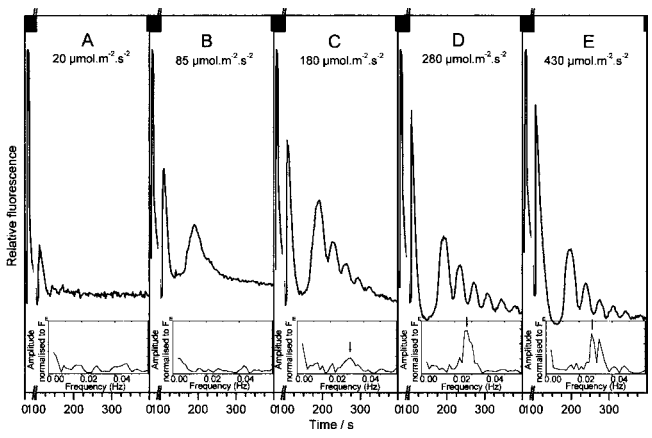

Figure 5. Irradiance dependence of oscillations in a palisade mesophyll cell of *T. caerulescens* in air. The fluorescence transients were recorded by exposing the sample to increasing irradiances with 5 min (after 20 and 85 $\mu mol \cdot m^{-2} \cdot s^{-1}$) to 10 min (after higher irradiances) dark relaxation between the individual measurements. The inserts show the FFT frequency spectra of the oscillatory part of the transients (after removal of offset and exponential trend). The arrows in the FFT inserts indicate the dominant (edge) frequency.

Influence of irradiance and gas composition. As in intact leaves, the optimum irradiance in isolated protoplasts was found to be around 300 $\mu mol \cdot m^{-2} \cdot s^{-1}$ in air. Enrichment with low concentrations of CO_2 reduced damping and shifted the optimum irradiance upward. However, the optimum of the enhancement (increased amplitude and decreased damping) was not around 1% CO_2 as in leaves (see above), but varied among the individual preparations from 0.5% to 2% CO_2. Most likely, this was caused by the limited and not fully reproducible diffusion toward the protoplasts through the layer of agarose.

Studies with sugars and inhibitors. Earlier studies (14) had suggested that oscillations are related to sugar transport between the mesophyll cells. Therefore, some of the oscillating protoplast preparations were first measured twice in the isolation medium. Afterwards, the latter was replaced by a medium in which the 0.8 *M* sorbitol was replaced by either 0.8 *M* glucose or 0.8 *M* sucrose. Even after 10–60 min of this treatment no significant changes of the oscillations could be observed (data not shown). In contrast, addition of 40 µ*M* glyceraldehyde suppressed the oscillations completely. Glyceraldehyde is known (33) to inhibit the Rubisco.

DISCUSSION

The application of two-dimensional Chl fluorescence kinetic microscopy allowed an analysis of oscillations in intact leaves of higher plants on a single-cell level for the first time. In selected plant species highly reproducible patterns of long persisting oscillations were recorded, which allowed us to investigate systematically the influence of various factors. FFT and sequential fitting of frequencies was applied to the records of oscillations and allowed us to characterize them in exact quantitative terms.

The studied oscillations were "autonomous" (see Reijenga *et al.* [34]), initiated by the onset of actinic irradiance. Earlier studies of photosynthetic oscillations in leaves ([1,2] in comparison with [7,13,14]) have shown that there are two types of such oscillations that differ markedly by their frequency. Oscillations with periods lasting for many minutes (about 5–40 min) were ascribed to the control of photosynthesis related to movements of stomata (7).

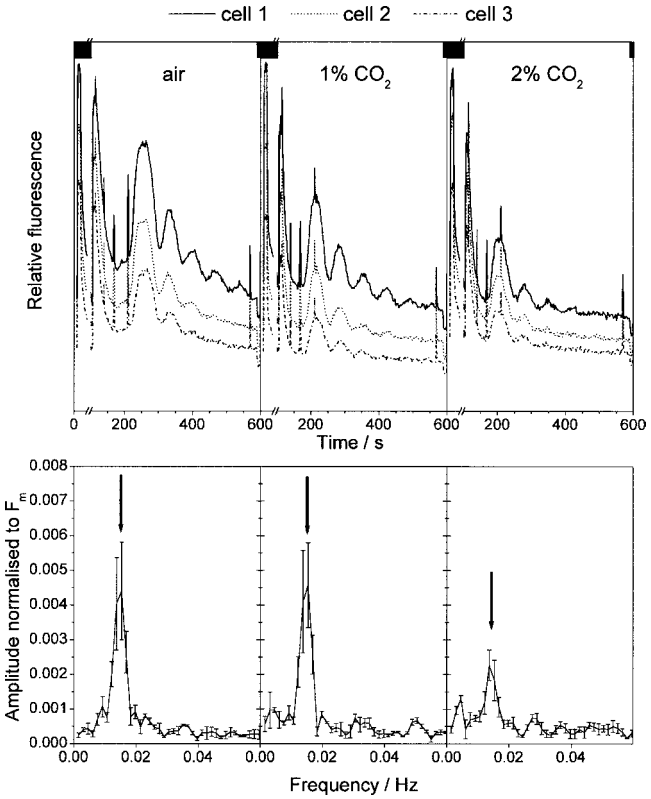

Figure 6. Influence of CO_2 on the frequency spectrum of oscillations in *T. caerulescens* at 180 $\mu mol \cdot m^{-2} \cdot s^{-1}$. Left, air; middle, 1% CO_2; right, 2% CO_2. Top, examples of fluorescence kinetics. Sharp spikes in fluorescence transients show F_m' measurements. Bottom, FFT spectra after the removal of offset and exponential trend. The FFT spectra were calculated from the time of the beginning of the m-peak until the end of actinic light exposure; their values represent the average (and the vertical bars the standard errors) between the cells of which also the kinetic traces are shown. The arrows indicate the dominant (edge) frequency.

Faster oscillations characterized by periods shorter than 2 min have not yet been unequivocally interpreted, but various biochemical and transport processes have been proposed for this mechanism as described in the Introduction. Because our records were limited to 10 min this article deals mainly with the properties of the short-period oscillations, but the mathematical analysis indicated that also the slow-period oscillations were present in our records. The most important result revealed by the mathematical analysis is, however, that the frequency spectrum of oscillations often consists of a higher number of oscillation frequencies, especially in the short-period group. This indicates that the oscillations are not due to only one mechanism (oscillating process in the cell) as assumed in the various present models (15–17,19,20). If it were so, then the short-period oscillations should be confined to only one frequency. The occurrence of the several peaks in the FFT spectra shown here cannot be explained by a nonlinearity of the relationship between photosynthesis and fluorescence or any other nonharmonic distortion of the kinetics, for several reasons. (1) The fitting (Fig. 2) showed that the kinetics can very accurately be described by a few sine functions (harmonic components), each representing a peak in the FFT spectrum. If the oscillations in fluorescence would not consist of such harmonic components, a much larger number of components would be needed to get a reasonable fit of the data. (2) Sometimes the presence of several frequencies was even visible with the bare eye, without any Fourier transform or fitting: at about

250, 340, 440 and 550 s in Fig. 2 there are clearly interference patterns that cannot possibly be caused by a single oscillation frequency. Thus it seems very likely that several of the mechanisms that have each been proposed to be the only cause of photosynthetic oscillations actually occur together. Besides the main hypotheses for mechanisms of short-period photosynthetic oscillations as mentioned already, a theoretical study of Ryde-Pettersson (18) even suggested 20 possible oscillators (all of them two-reactant interactions related to the Calvin cycle) that could contribute to photosynthetic oscillations. As an alternative to several independent processes oscillating in parallel, it is also possible that each of the oscillation frequencies corresponds to a process in a sequence of events. For example, the mechanisms converting the oscillations in carbon fixation to changes in Chl fluorescence could themselves be oscillatory. To distinguish between these possibilities is an important question for further research.

Several authors have suggested that oscillations originate from cell–cell interactions. Siebke and Weis (14) have proposed such interactions in the form of sugar transport because they observed that the distribution of oscillation parameters such as frequency, amplitude and damping reflected the minor vein distribution. The present study, however, yielded different results. First, the heterogeneity observed at low oscillation inducing irradiance was on the scale of individual cells and did not reflect the distribution of minor veins. At high irradiances the oscillations in our measurements were almost completely synchronous for the whole measured area. Furthermore, if sugar transport directly influenced oscillations, they should be modified by an addition of high concentrations of these sugars to the cells. In the present study, oscillations in protoplast suspensions with and without sucrose or glucose addition were identical.

Siebke and Weis (13,14) have suggested that the oscillating area units are the alveoli, and consequently heterogeneity should occur mainly in heterobaric leaves. The leaves of the *Thlaspi* species are not heterobaric, but nevertheless their mesophyll cells displayed oscillations. These oscillations differed in their properties for areas that are much smaller than the average size of alveoli. At the lowest oscillation inducing irradiances, even oscillations in neighboring cells could have strongly different phases and damping. This observation pointed at a determination of oscillation properties inside the single cells. The latter has been proven by analyzing oscillations of isolated protoplasts in suspension. Neighboring protoplasts under completely identical external conditions often drastically differed in all oscillation parameters, *i.e.* frequency, damping and maximum amplitude. Therefore, differences in the microenvironment around individual cells in a tissue (gas conditions, supply of sugars and water, *etc.*) cannot be the direct reason of oscillation heterogeneity. The different behavior of different cells is, most likely, a property of the cells themselves connected to different expression levels of the enzymes involved in oscillations. Thus, our results offer a partial proof of a hypothesis formulated by Siebke and Weis (14). In discussing the disparate oscillatory characteristics of mesophyll cells differing by their position relative to minor leaf veins they wrote: ''One may expect differential adjustments of cells at the transcription level along the sugar transport pathway between the veins.'' Although in our case the heterogeneity was not reflecting the vein distribution, our results support the concept that oscillations are determined by the enzymatic outfit of individual cells.

In our experiments the oscillations were triggered only when a proper balance was attained between the irradiance applied and the ambient concentration of CO_2. The optimum values of both factors are specific for the given object. These results are in line with earlier studies, which suggested that oscillations are initiated and supported by imbalances between the photosynthetic light reactions

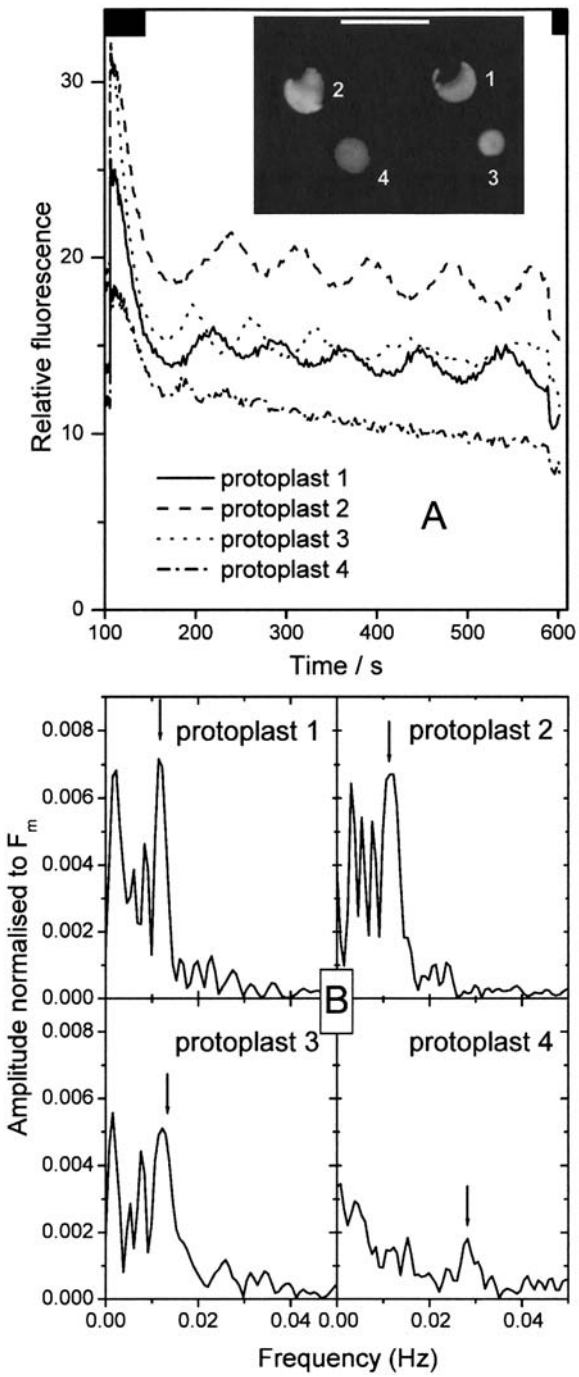

Figure 7. Oscillations in isolated *T. caerulescens* protoplasts at 410 $\mu mol \cdot m^{-2} \cdot s^{-1}$. The protoplasts were fixed in 1% ultra-low-melting agarose perfused with isolation medium that was saturated with air enriched with 2% CO_2. Heterogeneity between individual protoplasts as shown by fluorescence kinetics (A) and FFT spectra after the removal of offset and exponential trend (B). The FFT spectra were calculated from the time of the beginning of the m-peak until the end of actinic light exposure. The arrows in the FFT spectra indicate the dominant (edge) frequency. The image shows the total fluorescence of the selected protoplasts during F_p (white bar = 50 μm).

and the Calvin cycle (11). On the other hand our observation that the visible oscillation frequency is neither directly correlated to the CO_2 concentration nor to irradiance shows that this frequency is not controlled by the rate of carbon fixation in the Calvin cycle.

Acknowledgements—The authors are most grateful to Ivan Šetlík for helpful advice throughout the project. Also, we would like to thank Mechtheld Blake-Kalff for help with setting up the method of isolating protoplasts, Steve McGrath and Sarah Dunham for kindly providing seeds of the plants, Anna Ruprechtová and Marie Šimková for germination of the seeds and T. Macho for precision mechanical work on the FKM. Critical reading of the manuscript by Steve Halperin and Martin Spiller is also gratefully acknowledged. This research was supported by grants from the Ministry of Education of Czech Republic (LN00A141 and MSM12310001) and by project AV0Z6087904 of the Institute of Landscape Ecology, ASCR. H. Küpper was supported by a fellowship from Studienstiftung des Deutschen Volkes and a grant of the Deutsche Forschungsgemeinschaft. We are grateful for material support from the Degussa-Hüls AG (Marl, Germany).

REFERENCES

1. Van der Veen, R. (1949a) Induction phenomena in photosynthesis. I. *Physiol. Plant* **2**, 217–234.
2. Van der Veen, R. (1949b) Induction phenomena in photosynthesis. II. *Physiol. Plant* **2**, 287–296.
3. Barrs, H. D. (1971) Cyclic variations in stomatal aperture, transpiration and leaf water potential under constant environmental conditions. *Annu. Rev. Plant Physiol.* **22**, 223–236.
4. Walker, D. A. (1992) Concerning oscillations. *Photosynth. Res.* **34**, 387–395.
5. Giersch, C. (1994) Photosynthetic oscillations: observations and models. *Comm. Theor. Biol.* **3**, 339–362.
6. Wilson, A. T. and M. Calvin (1955) The photosynthetic cycle. CO_2 dependent transients. *J. Am. Chem. Soc.* **77**, 5948–5957.
7. Raschke, K. (1965) Die Stomata als Glieder eines schwingungsfähigen CO_2-Regelsystems. Experimenteller Nachweis an *Zea mays* L. *Z. Naturforsch.* **20B**, 1261–1270.
8. Barrs, H. D. and B. Klepper (1968) Cyclic variations in plant properties under constant environmental conditions. *Physiol. Plant* **21**, 711–730.
9. Walker, D. A., M. N. Sivak, R. T. Prinsley and J. K. Cheesbrough (1983) Simultaneous measurement of oscillations in oxygen evolution and chlorophyll a fluorescence in leaf pieces. *Plant Physiol.* **73**, 542–549.
10. Ogawa, T. (1982) Simple oscillations in photosynthesis of higher plants. *Biochim. Biophys. Acta* **681**, 103–109.
11. Laisk, A., K. Siebke, U. Gerst, H. Eichelmann, V. Oja and U. Heber (1991) Oscillations in photosynthesis are initiated and supported by imbalances in the supply of ATP and NADPH to the Calvin cycle. *Planta* **185**, 554–562.
12. Veljovic-Jovanovic, S. and Z. G. Cerovic (1991) Induction of oscillations in chlorophyll fluorescence by re-illumination of intact isolated pea chloroplasts. *Planta* **185**, 397–400.
13. Siebke, K. and E. Weis (1995a) Assimilation images of leaves of *Glechoma hederacea*: analysis of non-synchronous stomata related oscillations. *Planta* **196**, 155–165.
14. Siebke, K. and E. Weis (1995b) Imaging of chlorophyll-a-fluorescence in leaves: topography of photosynthetic oscillations in leaves of *Glechoma hederacea. Photosynth. Res.* **45**, 225–237.
15. Giersch, C. (1986) Oscillatory response of photosynthesis in leaves to environmental perturbations: a mathematical model. *Arch. Biochem. Biophys.* **245**, 263–270.
16. Laisk, A. and D. A. Walker (1986) Control of phosphate turnover as a rate-limiting factor and possible cause of oscillations in photosynthesis: a mathematical model. *Proc. R. Soc. Lond. B* **227**, 281–302.
17. Laisk, A. and H. Eichelmann (1989) Towards understanding oscillations: a mathematical model of the biochemistry of photosynthesis. *Phil. Trans. R. Soc. Lond. B* **323**, 369–384.
18. Ryde-Pettersson, U. (1991) Identification of possible two-reactant sources of oscillations in the Calvin photosynthesis cycle and ancillary pathways. *Eur. J. Biochem.* **198**, 613–619.
19. Buschmann, P. and D. Gradmann (1997) Minimal model for oscillations of membrane voltage in plant cells. *J. Theor. Biol.* **188**, 323–332.
20. Walker, D. A. and M. N. Sivak (1985) Can phosphate limit photosynthetic carbon assimilation *in vivo*? *Physiol. Vég.* **23**, 829–841.
21. Fridlyand, L. E. (1998) Independent changes of ATP/ADP or ΔpH could cause oscillations in photosynthesis. J. Theor. Biol. 193, 739–741.
22. Raschke, K. (1975) Stomatal action. *Annu. Rev. Plant Physiol.* **26**, 309–340.
23. Weis, E. and J. A. Berry (1987) Quantum efficiency of photosystem II in relation to 'energy'-dependent quenching of chlorophyll fluorescence. *Biochim. Biophys. Acta* **894**, 198–208.
24. Genty, B., J.-M. Briantais and N. R. Baker (1989) The relationship between the quantum yield of photosynthetic electron transport and quenching of chlorophyll fluorescence. *Biochim. Biophys. Acta* **990**, 87–92.
25. Cardon, Z. G., K. A. Mott and J. A. Berry (1994) Dynamics of patchy stomatal movements, and their contribution to steady-state and oscillating stomatal conductance calculated using gas-exchange techniques. *Plant Cell Environ.* **17**, 995–1007.
26. Eckstein, J., W. Beyschlag, K. A. Mott and R. Ryel (1996) Changes in photon flux can induce stomatal patchiness. *Plant Cell* **19**, 1066–1074.
27. Küpper, H., I. Šetlík, M. Trtílek and L. Nedbal (2000a) A microscope for two-dimensional measurements of *in vivo* chlorophyll fluorescence kinetics using pulsed measuring light, continuous actinic light and saturating flashes. *Photosynthetica* **38**, 553–570.
28. Baker, A. J. M., R. D. Reeves and A. S. M. Hajar (1994) Heavy metal accumulation and tolerance in British populations of the metallophyte *Thlaspi caerulescens* J.&C. Presl (Brassicaceae). *New Phytol.* **127**, 61–68.
29. Küpper, H., E. Lombi, F.-J. Zhao and S. P. McGrath (2000b) Cellular compartmentation of cadmium and zinc in relation to other elements in the hyperaccumulator *Arabidopsis halleri*. *Planta* **212**, 75–84.
30. Shen, Z. G., F.-J. Zhao and S. P. McGrath (1997) Uptake and transport of zinc in the hyperaccumulator Thlaspi caerulescens and the non-hyperaccumulator Thlaspi ochroleucum. *Plant Cell Envir.* **20**, 898–906.
31. Coleman, J. O. D., R. Randall and M. M. A. Blake-Kalff (1997) Detoxification of xenobiotics in plant cells by glutathione conjugation and vacuolar compartmentalization: a fluorescent assay using monochlorobimane. *Plant Cell Env.* **20**, 449–460.
32. Nedbal, L., J. Soukupová, D. Kaftan, J. Whitmarsh and M. Trtílek (2000) Kinetic imaging of chlorophyll fluorescence using modulated light. *Photosynth. Res.* **66**, 3–12.
33. Stokes, D. M. and D. A. Walker (1972) Photosynthesis by isolated chloroplasts. Inhibition by D,L-glyceraldehyde of carbon dioxide assimilation. *Biochem. J.* **128**, 1147–1157.
34. Reijenga, K., H. Westerhoff, B. Kholodenko and J. Snoep (2002) Control analysis for autonomously oscillating biochemical networks. *Biophys. J.* **82**, 99–108.